Fachtagung "Experimentelle Strömungsmechanik"
5.–7. September 2023, München

Concentration Measurements based on Particle Imaging

Konzentrationsmessungen basierend auf Partikelbildgebung

Abhilash Sankaran, Rainer Hain, Christian J. Kähler
Universität der Bundeswehr München,
Institute of Fluid Mechanics and Aerodynamics

Particle concentration, Diffusion, Voronoi Cells, Exponential moving average
Partikelkonzentration, Diffusion, Voronoi-Zellen, Exponentieller gleitender Durchschnitt

Abstract

The objective of this study is to expand the application of the Particle Image Velocimetry (PIV) method to include the determination of particle concentration within the visualized window, in addition to providing velocity information. The analysis of different particle image-based concentration methods is presented. Specifically, two techniques: a) an exponential averaging method; and b) Voronoi cell based method; are applied on the particle images.
Exponential averaging method is a simple technique which could be easily applied to the particle images with a constant length scale for the sliding average. However, the fixed length scale could lead to broadened interface or "marker-shot" like effect at low concentrations. So, for scenarios involving highly non-uniform distribution of the particles that can occur in different flow fields of practical importance like concentrated jet issuing into ambient, one would need additional effort for reliable detection of the interface. Voronoi cell based concentration determination technique has the advantage that the resolution is spatially adaptive to the varying concentration. The technique could also be applied where the interface determination is also important.
For a comprehensive analysis, synthetic particle images were generated to simulate a diffusion problem with an initial step in concentration distribution. The aforementioned techniques were applied and compared using this synthetic test case. Furthermore, an experimental case involving a turbulent puff was considered as an example. In this experimental scenario, a calibration function is determined with respect to particle counter measurement to obtain the physical particle concentration.

Introduction

In many fluid mechanical systems, the concentrations of the species are time or space dependent or both. Concentration field measurements are useful to understand the spatial distribution of the particle concentration in various scenarios including detection of boundaries of the species, mixing effectiveness to name a few (Gnirß and Tropea, 2008). Typical methods involve point measurement sensor system which does not give spatial information. However, most point measurement systems like particle counter samples the part of the air to count the particles. This is, in addition to being intrusive to the system being measured, could only provide an average in longer duration of the test.

GALA e.V., Karlsruhe, Germany, ISBN 978-3-9816764-9-5

One image-based method proposed before is based on intensity of the scattered laser light from particles. However, the method involves many corrections to arrive at physical concentration. Here, methods involving direct counting of the particles in the images are presented. One of the methods followed here is to apply an exponential sliding average method for concentration determination. It needs to be noted that the length scale is fixed once chosen and cannot be varied within the image even if the concentration of the particles could be drastically different. Another method applied here is method based on Voronoi cells, which in principle is an adaptive grid procedure to calculate the local particle concentration. Such method has been demonstrated for application in the cosmological application(Schaap and Van De Weygaert, 2000).

Particle Concentration Measurement

This study primarily focuses on the particle image based concentration measurement based on two techniques: a) sliding average method; b) Voronoi cell based method.

Sliding average Method: This is the exponential moving average type filter applied in Davis. This method applies a local filter to compute the average particles per pixel as (LaVision, 2021)

$$P^{avg}(i) = \left(1 - \frac{1}{l}\right) P^{avg}(i-1) + \left(\frac{1}{l}\right) P(i) \quad (1)$$

where $P(i)$ is the intensity at a certain pixel i, P^{avg} is the computed value at pixel i and $i-1$ accordingly. l is the length scale in pixel chosen for the average computation. The same method is applied in all four directions one after the other to compute the sliding average value of the intensity values.
The result obtained by the sliding average method with one particle at 0,0 is shown in figure 1 with different length scales chosen. It needs to be noted that the value at 0,0 before the application of the sliding average is 1, i.e. 1 particle at the center pixel (1 ppp). The method effectively distributes the particle into all four directions on each pass as given by eq.(1). For example at length scale l = 4 px, the peak value is C_l ~ 0.02 ppp at the center and reduces to effectively 0 far from the length scale defined. The peak value decreases as the length scale for averaging is increased. While, the extent of the effect of the particle increases as the length scale is increased.

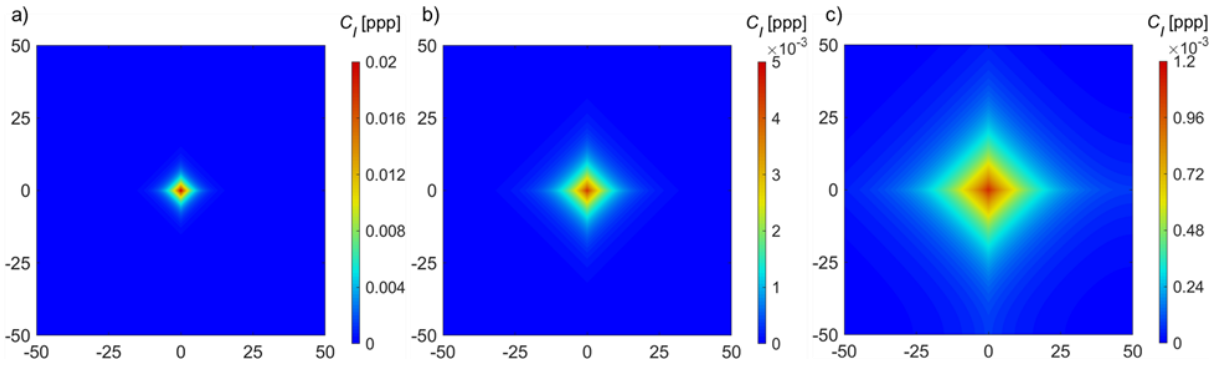

Figure 1: The contour of the variation of the local C_l value with one particle (at 0,0) for different length scale for the sliding average: (a) l = 4 pixels; (b) l = 8 pixels; (c) l = 16 pixels.

Voronoi cell based method: Voronoi cell around a point (or particle) is the polygonal region around it that is close to the point and not any other point which form a closed network with other cells around without any overlaps and without any gaps or holes (see Schaap and Van

GALA e.V., Karlsruhe, Germany, ISBN 978-3-9816764-9-5

De Weygaert, 2000). An example with uniformly spaced particles with different spacing in either side of origin is shown in figure 2.
The inverse of the cell area technically represents the number of particles per unit area, which can be interpreted as particle density or concentration. However, it is important to note that this measure does not necessarily reflect concentration in the traditional continuum sense, as it focuses on individual particles and continuum definition no longer holds. To address this, it becomes necessary to approximate the continuum by either considering a sufficiently large number of particles or selecting an appropriate examination window size. Here, the concentration is calculated as the inverse of average of *K* nearest neighbor cells.

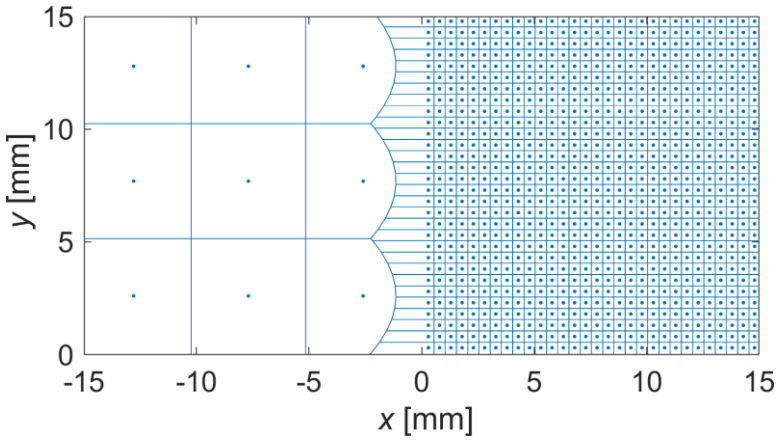

Figure 2: The Voronoi cells around uniformly spaced particles with concentrations C_1 = 3.84×10^{-4} 1/cm^2 and C_2 = 0.04 1/cm^2 to the left and right of origin respectively.

Results and Discussion with Synthetic Case

For comparison of the different methods, firstly a synthetic case of diffusion problem is considered. A domain extending from -250 mm < *x* < +250 mm and 0 < *y* < +25 mm is considered. The ends at *x* axis are closed by walls. At *x* = 0, there is a removable wall, which is removed at *t* = 0. A repeating boundary condition is considered along the *y*-axis. Before the start, a uniformly placed particles with C_1 = 3.84×10^{-4} 1/cm^2 and C_2 = 0.04 1/cm^2 is considered at left (*x*<0) and right (*x*>0) of origin respectively (figure 2). The diffusion process is modelled with applying diffusion jumps to each particle in the domain.
The diffusion jump of the particles Δr in a time step Δt could be found as (Daune, 1999;Sankaran et al., 2020):

$$\Delta r = 2\sqrt{D\Delta t \log\left(\frac{1}{R}\right)} \tag{2}$$

where, R is a random number between 0 and 1 defining the probability of the diffusion jump of length Δr. This jump Δr occurs in random direction θ with $0 \leq \theta \leq 2\pi$. A diffusion coefficient of D = 10^{-5} m^2/s is assumed here and time step of 1 s is considered.
The diffusion process is run for long time before time *t* = 0 resulting in a practical uniform concentration in both sides of the origin as shown in figure 3a. At *t* = 0, the wall separating the two concentration side is removed.
For time scales $t << L^2/D$ (where *L* = 250 mm, is the distance from center to the side walls), one can compare the distribution to the analytical solution in one dimension having an initial step in concentration. The solution for diffusion from *t* = 0 (i.e. after the wall separating region is removed), the analytical solution is given by (Balluffi et al., 2005)

GALA e.V., Karlsruhe, Germany, ISBN 978-3-9816764-9-5

$$C = (C_2 - C_1)\left(\frac{1}{2} + \frac{1}{2}\mathrm{erf}\left(\frac{x}{\sqrt{4Dt}}\right)\right) + C_1 \quad (3)$$

One can test the capturing of the initial step with the methods detailed above. This gives the information on the characteristics of the interface determination by the method employed. The practical initial step distribution before the interaction between the two different concenctration obtained at t = 0 is shown in figure 3a. The voronoi cells constructed for the corresponding distribution is shown in figure 3b. Note that for Voronoi cell construction, a reflective boundary condition is applied for all the sides and the corners resulting in 8 repetitions of the window of interest. This is to have the cells of appropriate size within the window of interest as the end points lead to open Voronoi cells (cells which are not closed within the boundary of interest).

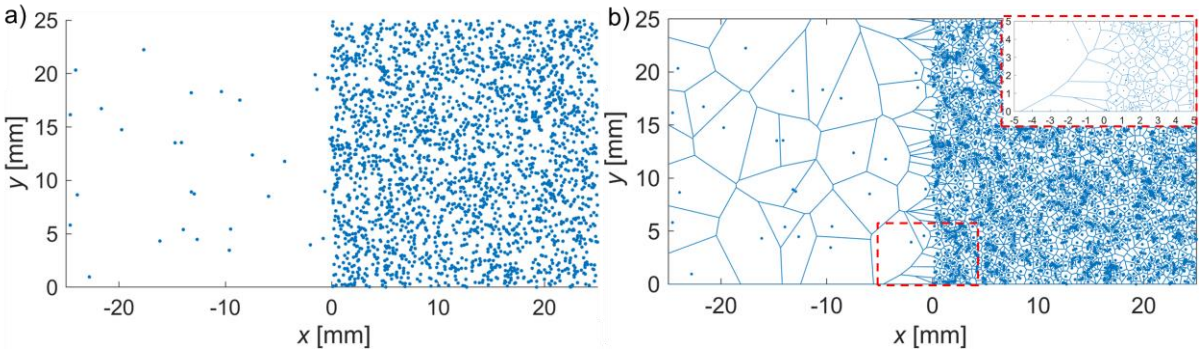

Figure 3: The initial distribution of the particles at t = 0, with the concentration of C_1 = 3.84×10^{-4} 1/cm^2 and C_2 = 0.04 1/cm^2 to the left and right of origin respectively. (b) Voronoi cells around this initial distribution and the inset shows a zoomed in view.

The comparison of the two methods applied to the instance t = 0 for the distribution shown in figure 3 is given in figure 4 (line at y = 12.5 mm is taken for comparison. The points are spaced at 1 mm along this line).

It shows that the Voronoi method reveals all the features at very small scales leading to large fluctuations at high concentrations. However, at the lower concentration, the variation appears lower (It needs to be noted that on a relative to their average values they are not that drastic). In case of the sliding average method with length scale of 1.6 mm, one can observe that the higher concentration is much more smoothened and the step change is also captured with a similar resolution as Voronoi method with K = 10. However, at low concentration, one can see a marker-shot like noise with values falling near zero and peaking at intervals. Hence, the length scale though is reasonable to capture the step and high concentration, at low concentration, it is not that suitable.

Another extreme would be to increase the number of cells averaged for the Voronoi method and increase the length scale for the sliding average method. Such cases are shown in figure 5. Here, the fluctuations to the local values in case of Voronoi method have improved. However, the limiting factor is that the values might lead to inappropriate values at the jump and at lower concentration when considering high number of particles with no regard to the physical length of the distribution. It is interesting to note that the smoothening of the jump is more towards the lower concentration; however, at the higher concentration it has not smoothened due to the data from 100 points still within a small physical scale. The sliding average method also shows that the concentration at the lower values is reasonable. However, again, the finer features are smeared as visible with the extent of the smoothening of the jump in concentration both on higher and lower concentration side.

GALA e.V., Karlsruhe, Germany, ISBN 978-3-9816764-9-5

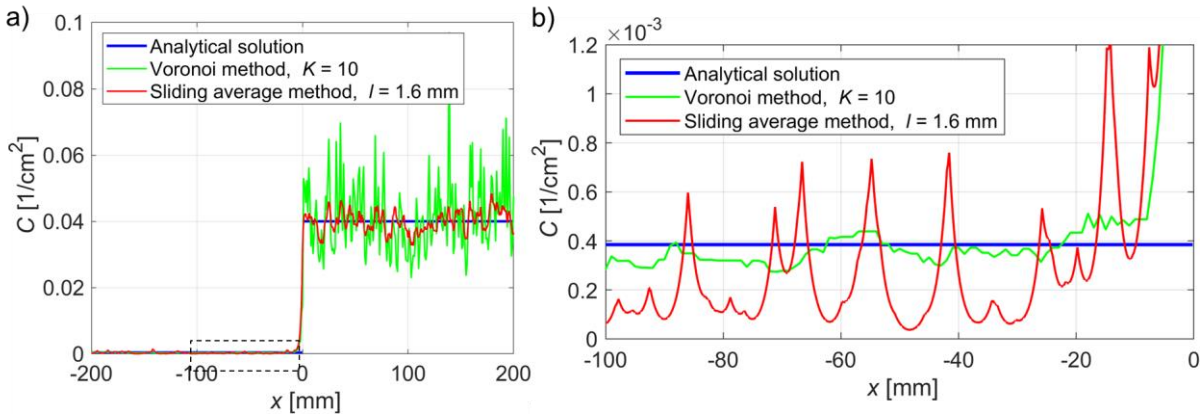

Figure 4: (a) Particle density distribution at t = 0 along the line y = 12.5 mm, comparing for the Voronoi method with K = 10, and sliding average method with l = 1.6 mm, and the analytical solution. (b) The zoomed-in view at the lower concentration region

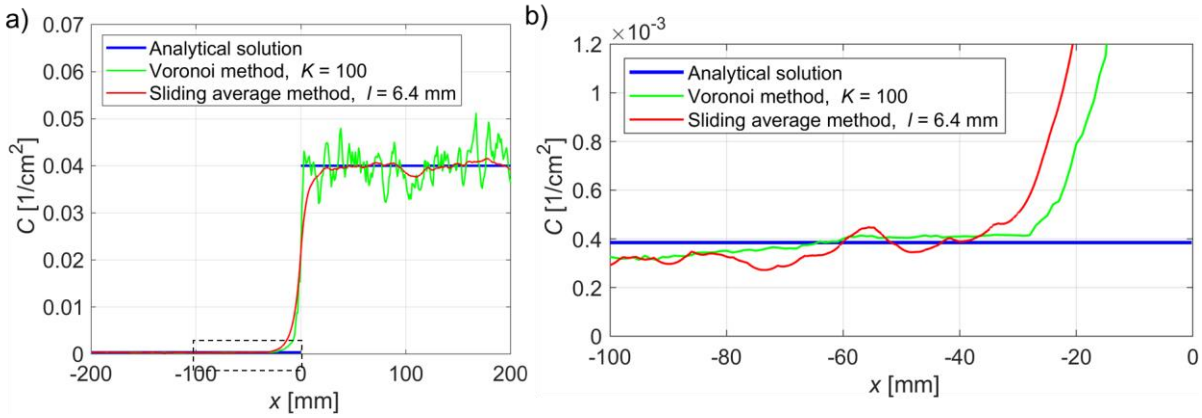

Figure 5: (a) Particle density distribution at t = 0 along the line y = 12.5 mm, comparing for the Voronoi method with K = 100, and sliding average method with l = 6.4 mm, and the analytical solution. (b) The zoomed-in view at the lower concentration region.

A possible solution which can be easily implemented for Voronoi method is to incorporate a criterion involving both a minimum number of particles and minimum length scale. Therefore, the averaging of the Voronoi cells is considered such that there is a minimum of K_{min} cells (say K_{min} = 10). In addition, if the length scale of K cells is smaller than the minimum length scale chosen (say a required resolution), then average the cell area within the minimum length scale. The obtained distribution with this adaptive Voronoi method and analytical solution for t = 0 and t = 50 s is presented in figure 6 and 7 respectively.
The results show that the adaptive method can capture the jump in concentration, while also giving control over how finer details need to be resolved. Further, the marker-shot noise effect is also avoided with accounting for only K = 10 cells.

GALA e.V., Karlsruhe, Germany, ISBN 978-3-9816764-9-5

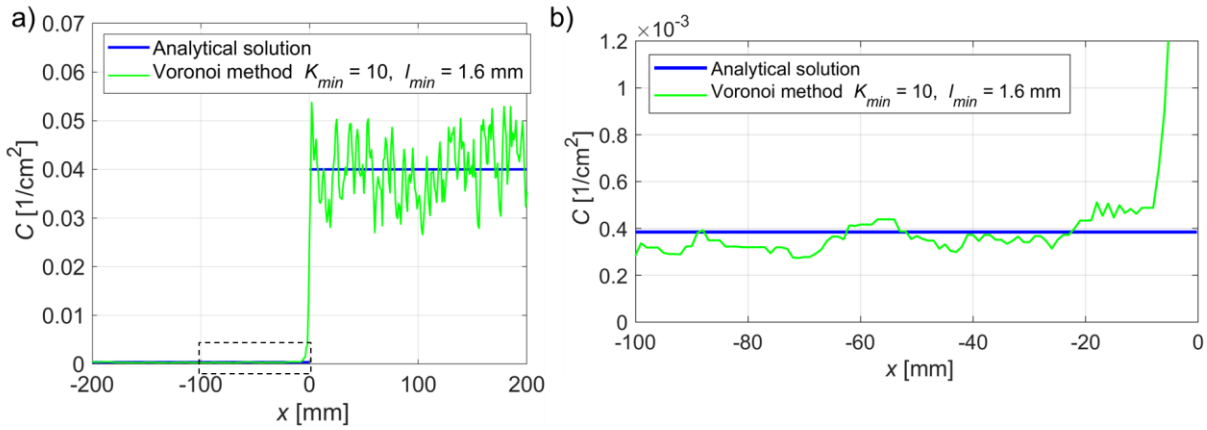

Figure 6: (a) Particle density distribution at t = 0 along the line y = 12.5 mm, applying the adaptive Voronoi method with K_{min} = 10 and l_{min} = 1.6 mm, and the analytical solution. (b) The zoomed-in view at the lower concentration region.

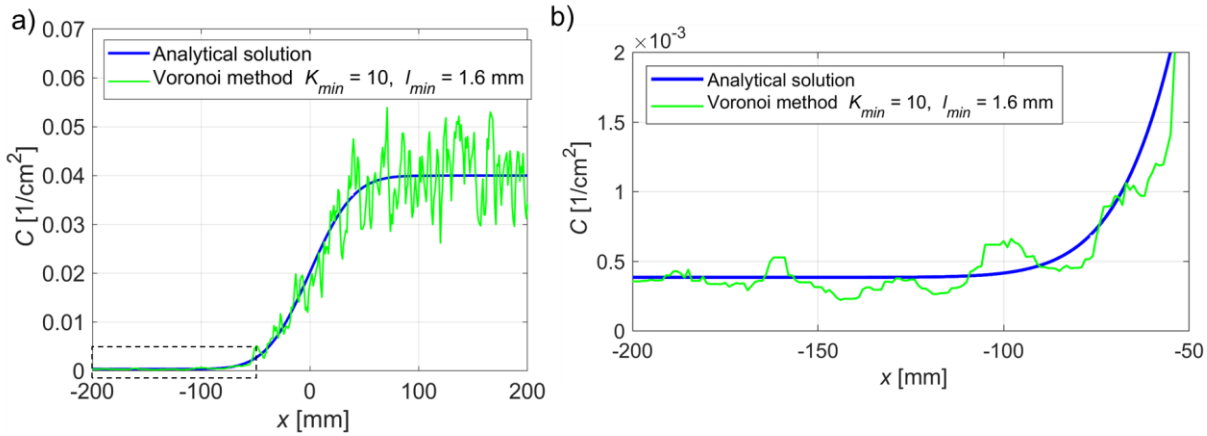

Figure 7: (a) Particle density distribution at t = 50 s along the line y = 12.5 mm, applying the adaptive Voronoi method with K_{min} = 10 and l_{min} = 1.6 mm, and the analytical solution. (b) The zoomed-in view at the lower concentration region.

Experimental Results

A pulsatile jet of air nebulized with DEHS particles (mean diameter ≈ 0.4 µm) into a closed room is visualized as an example case with concentration variation. The air is heated through water bath maintained at 37 °C and led to the source of circular cross section of diameter 3 cm. The measurement equipment includes the two cameras, the laser, and the computer for stereo PIV system. The air is compressed by displacement method which could be controlled to provide a definite volume of air at a defined frequency. The PIV images are also taken at specified phase of the frequency, so that the results could be phase averaged.

The measuring system was controlled by the DaVis 10 software from LaVision GmbH, which was also utilized for data evaluation in addition to MATLAB. The concentration measurements were conducted with the cameras in forward scattering mode. The cameras are angled with respect to the laser sheet plane. Stereoscopic PIV calculations are conducted with the particle images from both the cameras.

The obtained velocity field V (absolute velocity magnitude) for the case with a total volume of 1000 mL and 16 cycles/minute is shown in figure 8.

GALA e.V., Karlsruhe, Germany, ISBN 978-3-9816764-9-5

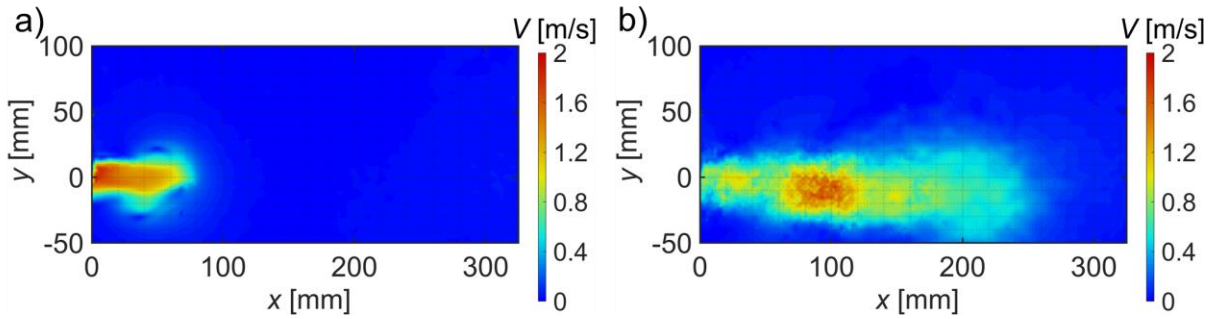

Figure 8. Average velocity magnitude (averaged with 10 cycles) contour at time instances: (a) *t'* (non dimensionalized by the cycle time), and (b) *t'* + 0.133. Cycle time = 3.75 s.

Further, the motivation of the present work is the determination of the concentration field utilizing the same data from the PIV particle images. For this, the calibration of the particle image data to the physical concentration is needed to account for the spatial variation of the laser intensity. For concentration calibration, separate sets of particle images are taken with uniform concentration in the room and simultaneous measurement using the particle counter as reference. This revealed non-linearity in dependence of the observed particles per pixel to the physical concentration as shown in figure 9. A smoothing spline fit is obtained for all points in the *x*-*y*-plane as a function of concentration as shown in figure 9.

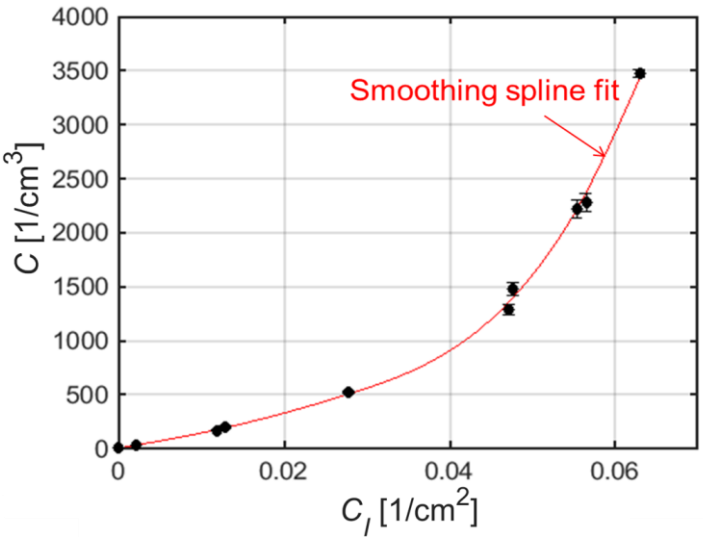

Figure 9. The smoothing spline fit obtained for a point at different uniform concentration. (Note that 0,0 point is added as a theoretical number density as they are not practically "measured")

It can be observed that the image particle density C_I increases linearly with physical concentration of particles until approximately 500 1/cm^3. However, with further increase in physical concentration, the image based particle density increase is gradual. This indicates the effect of the particle overlaps in the observed images. Further, similar procedure is repeated for the Voronoi cell method.

GALA e.V., Karlsruhe, Germany, ISBN 978-3-9816764-9-5

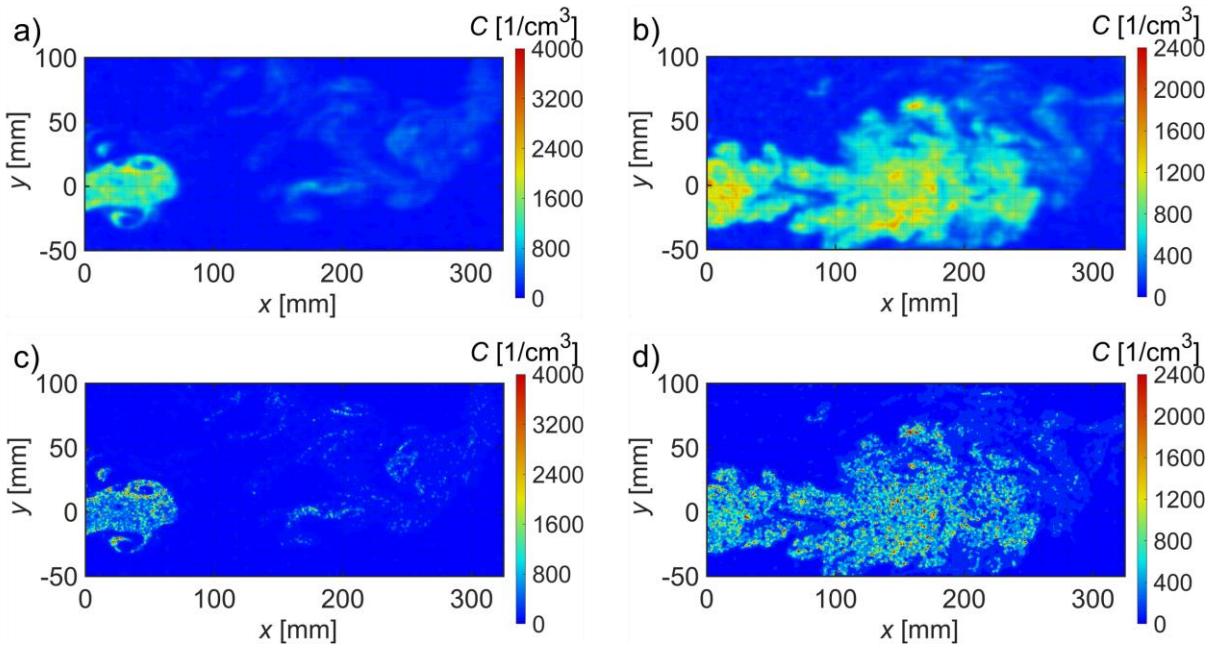

Figure 10. The concentration contour for the instances *t'* and *t'* + 0.133 (same instances as in velocity field in figure 8) obtained by (a) the sliding average method *I* = 16 pixel and (b) Voronoi cell method *K* = 5. Note that for the Voronoi method, the contour is plotted on the irregular grid formed by the particles.

The resulting concentration profile for the instantaneous PIV images for two time instances is shown in figure 10. Sliding average with *I* = 16 pixel and the Voronoi method with *K* = 5 is compared. It can be observed that qualitatively both the methods reveal similar structures on the larger scales. However, the Voronoi method reveals finer details.

Conclusion

This work focuses on the determination of particle concentration using particle images obtained from PIV. Specifically, two methods, namely the Sliding Average method and Voronoi Cell-based method, have been explored and analyzed. The characteristics and limitations of each approach are presented using synthetic data of a diffusion problem with an initial step in concentration. Additionally, an adaptive Voronoi method is introduced, which effectively captures all essential features, including the initial jump conditions, in a diffusion problem. This method provides flexibility in adjusting the physical length scale and minimum number of particles, which allows customization according to specific requirements.
Furthermore, the methods are applied to a real experimental turbulent puff. While the applied methods successfully reveal the primary concentration distribution, an additional consideration arises due to particle-particle overlap, which introduces non-linearity compared to the physical concentration. Nevertheless, the applied methods exhibit promise for real-case applications and the derivation of absolute concentration fields using particle images obtained from PIV.

Acknowledgements

This research is funded by dtec.bw – Digitalization and Technology Research Center of the Bundeswehr through project LUKAS which we gratefully acknowledge. dtec.bw is funded by the European Union – NextGenerationEU.

GALA e.V., Karlsruhe, Germany, ISBN 978-3-9816764-9-5

Literature

Balluffi, R. W., Allen, S. M., & Carter, W. C., 2005: "Kinetics of materials"**,** John Wiley & Sons, New Jersey.
Daune, M., 1999: "Molecular biophysics: structures in motion"**.**
Gnirß, M., Tropea, C., 2008: "Simultaneous PIV and concentration measurements in a gas-turbine combustor model ", Experiments in fluids, 45(4), 643-656
LaVision, 2021: Product Manual DaVis 10.2 Software", LaVision GmbH, Göttingen
Sankaran, A., Pawłowska, S., Pierini, F., Kowalewski, T. A., Yarin, A. L., 2020: “Dynamics of electrospun hydrogel filaments in oscillatory microchannel flows: A theoretical and experimental approach”. Physics of Fluids, 32(7), 072008.
Schaap, W. E., Van De Weygaert, R., 2000: "Continuous fields and discrete samples: reconstruction through Delaunay tessellations", arXiv preprint astro-ph/0011007

GALA e.V., Karlsruhe, Germany, ISBN 978-3-9816764-9-5